Received: 28 February 2019 | Revised: 30 March 2019 | Accepted: 10 April 2019
DOI: 10.37917/ijeee.15.1.4 | Vol. 15 | Issue 1 | June 2019
Open Access
Iraqi Journal for Electrical and Electronic Engineering
Original Article

Design and Implementation of Hybrid-Climbing Legged Robot

Mustafa Y. Hassan
Electrical Engineering Depart.
University of Basrah
Basrah, Iraq
engmustafaa95@gmail.com

Mofeed T. Rashid
Electrical Engineering Depart.
University of Basrah
Basrah, Iraq
Mofeed.t.rashid@ieee.org

Ali H. Abdulaali
Mechanical Engineering Depart.
University of Basrah
Basrah, Iraq
ali_alshaheen@yahoo.com

Abstract *In this paper, the hybrid-climbing legged robot is designed, implemented, and practically tested. The robot has four legs arranged symmetrically around the body were designed for climbing wire mesh fence. Each leg in robot has 3DOF which makes the motion of the robot is flexible. The robot can climb the walls vertically by using a unique design of gripper device included metal hooks. The mechanism of the movement is a combination of two techniques, the first is the common way for the successive movement like gecko by using four limbs, and the second depending on the method that used by cats for climbing on the trees using claws, for this reason, the robot is named hybrid-climbing legged robot. The movement mechanism of the climbing robot is achieved by emulating the motion behavior of the gecko, which helped to derive the kinematic equations of the robot. The robot was practically implemented by using a microcontroller for the mainboard controller while the structure of the robot body is designed by AutoCAD software. Several experiments performed in order to test the success of climbing on the vertical wire mesh fence.*

Index Terms**—climbing robot, legged robot, kinematic model, robot gripper.**

I. Introduction

The climbing robots that can climb on vertical surfaces (rocks, walls ... etc.) are used in dangerous places, in addition, for the environment that is difficult for humans to access. Therefore, there are several applications for these robots like civilian, military, industrial, scientific research purposes, guidance, and navigation ... etc. The design of the robot gripper structure is an important factor for enables robots to climb vertical surfaces such as stucco wall, wire mesh fence, and trees. The motion behavioral of gecko is a useful source for design climbing robot which the kinematic model of gecko limbs can be used as a good model for controlling climbing robot, in another hand, the mechanism of clamping on the vertical wall can be designed based on the mechanism of cat claws when it trying to cling to the wall.

There are several types of climbing robots that have the capability to climb on various surfaces depended on the design of arm and gripper device, types of surface, and mechanism of the movement during climb. Geckobot [1], Waalbot [2], and [3], using elastomer adhesives to attach to the wall. The robot that made from dry adhesive that can climb on flat and smooth walls such the stickybot III [4], Abigaille II [5], which uses polymeric stalks to adhesion to the wall exactly like gecko feet. The disadvantage of these types of robot is the surface must be clean and do not contain dust or water droplets. The researchers developed another type of climbing robot that dependent on limb and leg position algorithm, such as LEMUR II [6], which have four limbs, each limb include four degree of freedom (4DOF) that autonomously climb on the rock, which was pre-placed on the wall. The disadvantage of LEMUR is that climb on training wall. The robot foot location constrained to special points that arranged randomly on the wall. Other types of adhesive method by using permanent magnet adhesion such as [7, 8], where magnetic wheels are used. The disadvantage of this method is that this robot can climb only on iron surfaces. Another types of the climbing robot are that contain micro spines in their gripper device like the RiSE [9] and [10-13], these robot are very similar to insects. The RiSE uses six legs, 20 motors, and micro spines that arranged in each pad at the end of leg for more reliable and stable attached to the rough surfaces. The CLIBO robot [14], has four limbs, each limb contain four servomotors (AX-12). It is use hook like claw mechanism for attachment on rough surfaces. The mechanism of the movement like the human movement during climb the rocks or mountains. The CLIBO robot is expensive because it has 16-servo motors type AX-12. Other robots that using claw mechanism are [15-25], which the mechanism of the climbing on wall is depending on using claw. Some of the climbing robots that used claw have only one hook used to attached to the wall like [19–22], while there are robots have a gripper device that contain multi-hook [14–18]. The hook-like claw method is suitable method for climbing on rough surfaces, also claw method using in climbing on the tree or palm [26–28], or climbing on mesh fence wall [29].

In this paper, the design and implementation of the climbing robot are presented, which the motion mechanism of robot legs is dependent on motion behavior of gecko, while the clings mechanism of the robot on the wall is depending on cat cling mechanism by its limbs claws. The kinematic model is derived for robot limbs motion in order to control the position of robot legs. Several experiments are achieved by using a wall made from a wire mesh fence in order to test the climbing robot in this environment.

This paper is arranged as follow: in section II we discuss the overall design, forward and inverse kinematics model. In section III, the gripper device mechanism are explained and implemented. In section IV, Simulation and practical experiments are presented. Finally, in section V, the results of the experiments are discussed and there are some conclusions.

II. Modelling of The Climbing Robot

A. *Overall design of the robot*

The robot have four legs that arranged symmetrically around the body. The robot is divided into two main parts, two legs in the upper part and two in the lower, and the two parts are connected to the waist as shown in Fig. 1.

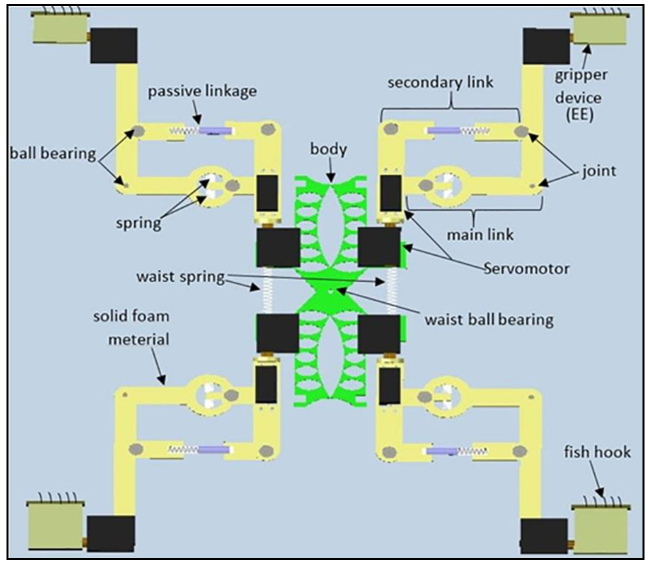

Fig. 1 Hybrid-climbing legged robot.

The two upper limbs are used to pull the robot to the upward and the other two lower limbs used to push the body upward. Each leg have 3DOF, which have active and passive joints. All 3DOF are motorized by using servomotor with metal gear which is characterized by high torque. The first DOF is M1 that located at the bottom of the arm and installed on the body, which considered non-moving relative to the arm. This motor have an axis parallel to the wall and responsible to move the whole arm inward/outward of the wall. This function is very important to generate a suitable distance away from the wall and thus prevent friction. The second DOF is M2, which is perpendicular to the wall, and it is responsible to move the arm forward so the whole robot is going up. M2 is connected to parallelogram linkage, which contain close and open chain link. The third DOF is M3, which is installed at the end of the arm (End Effector), which specialized for gripper device. This servo have two main essential functions, first, it is responsible to make a reliable and strong attachment to the wall, and the second function is to prevent friction of the arm against the wall.

B. *Forward Kinematics*

The forward kinematic analysis is the relationship between the joint angle of the robot manipulator and the position, orientation of the end effector. Denavit-Hartenberg (D-H) presented the kinematics model based on a 4x4 homogeneous transformation matrix that describes the position and orientation of the end effector frame with respect to the base frame [30], in this paper D-H algorithm is used to derive the kinematic model of the climbing robot arm. This kinematic model describes the position and orientation of the end effector with respect to the reference coordinate.

In general, the kinematic model is divided into two main sections, the transition from frame 0 to frame 3, which contain two chains SC1, and SC2, and transition from frame 3 to frame 5. In Fig. 2, the frame ($f_{3'}$) is affixed to the proximal end of the link (a_3) and the frame ($f_{3''}$) is affixed to the distal end of the link ($a_{2'}$). Both these frames represent the same point in Cartesian space.

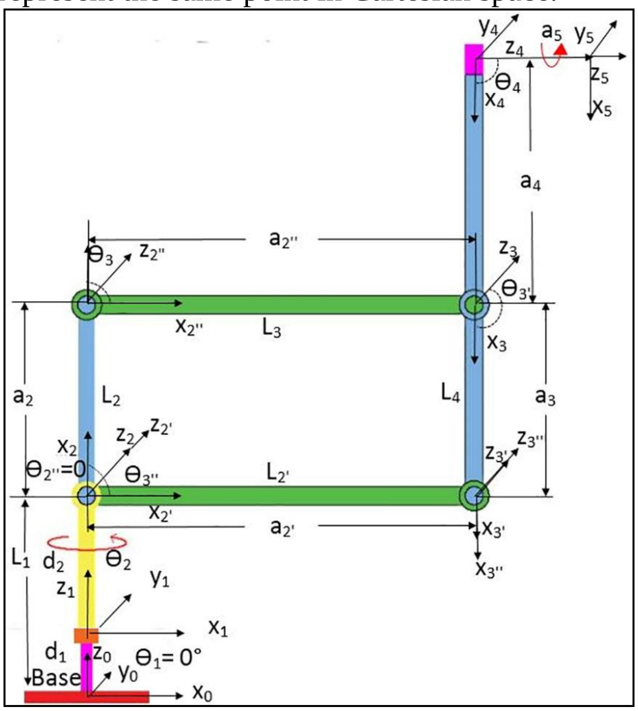

Fig.2 Development of kinematic model using D-H parameter method.

To transform the frame ($f_{3'}$) and ($f_{3''}$) to the base frame the path is divided into two serial chains SC1 and SC2. The chain SC1 consist of the link L_1, L_2, L_3, and L_4. By using D-H notation we can get

$$A^0_{3'}sc1 = A^0_1 * A^1_2 * A^2_{2''} * A^{2''}_3 * A^3_{3'} \tag{1}$$

From chain 4x4 transformation matrices of Eq. (1), we get

$$A^0_{3'}sc1 = \begin{pmatrix} C_2C_{33'} & -C_2C_{33'} & -S_2 & X^0_{3'} \\ S_2C_{33'} & -S_2S_{33'} & -C_2 & Y^0_{3'} \\ -S_{33'} & -C_{33'} & 0 & Z^0_{3'} \\ 0 & 0 & 0 & 1 \end{pmatrix} \tag{2}$$

$$P^0_{3'}sc1 = \begin{pmatrix} X^0_{3'} \\ Y^0_{3'} \\ Z^0_{3'} \end{pmatrix} = \begin{pmatrix} C_2 * (a_2 + a_3C_{33'} + a_{2''}C_3) \\ S_2 * (a_2 + a_3C_{33'} + a_{2''}C_3) \\ d_1 + d_2 - a_{2''}S_3 - a_3S_{33'} \end{pmatrix} \tag{3}$$

The chain SC2 consist of links L_1 and $L_{2'}$ so the frame $f_{3''}$ can be transformed to f_0, by using the same way that used in SC1 we can get

$$A^0_{3''}sc2 = A^0_1 * A^1_{2'} * A^{2'}_{3''} \tag{4}$$

$$A^0_{3''}sc2 = \begin{pmatrix} C_2C_{3''} & -C_2S_{3''} & -S_2 & X^0_{3''} \\ S_2C_{3''} & -S_2C_{3''} & C_2 & Y^0_{3''} \\ -S_{3''} & -C_{3''} & 0 & Z^0_{3''} \\ 0 & 0 & 0 & 1 \end{pmatrix} \tag{5}$$

and the position vector is

$$P^0_{3''}sc2 = \begin{pmatrix} X^0_{3''} \\ Y^0_{3''} \\ Z^0_{3''} \end{pmatrix} = \begin{pmatrix} a_{2'}C_2C_{3''} \\ a_{2'}S_2C_{3''} \\ d_1 + d_2 - a_{2'}S_{3''} \end{pmatrix} \tag{6}$$

Both equations (1) and (4) represent the same point in Cartesian space for the given values of D-H parameters.

Now, as reported by Siciliano et al., [31] for a closed loop robot having last joint as revolute ($f_{3'}$, $f_{3''}$), then a_3 and $a_{2'}$ are a fixed offset along axis z_3. The position constraints of a parallelogram linkage can be obtained as

$$\left(\left(P^0_{3'}sc1\right) - \left(P^0_{3''}sc2\right)\right) = \begin{pmatrix} X^0_{3'} \\ Y^0_{3'} \\ Z^0_{3'} \end{pmatrix} - \begin{pmatrix} X^0_{3''} \\ Y^0_{3''} \\ Z^0_{3''} \end{pmatrix} = \begin{pmatrix} 0 \\ 0 \\ 0 \end{pmatrix} \tag{7}$$

Substitute both Eq.(3) and Eq.(6) in Eq.(7) we get

$$C_2 * (a_2 + a_3C_{33'} + a_{2''}C_3) - a_{2'}C_2C_{3''} = 0 \tag{8}$$

$$S_2 * (a_2 + a_3C_{33'} + a_{2''}C_3) - a_{2'}S_2C_{3''} = 0 \tag{9}$$

$$d_1 + d_2 - a_{2''} S_3 - a_3 S_{33'} - (d_1 + d_2 - a_2 S_{3''}) = 0 \quad (10)$$

Where the vector of joint variables is q' = [θ_3 $\theta_{3'}$ $\theta_{3''}$] depend on three angles. From the parallelogram linkage (L_2, L_3, L_4, and $L_{2'}$), it is found that a_2 = a_3 and $a_{2'}$ = $a_{2''}$. Using this relationship and divided Eq.(8) on C_2 and Eq.(9) on S_2 respectively, the constraints can be simplified as

$$a_2 * (1 + C_{33'}) + a_{2'} * (C_3 - C_{3''}) = 0 \quad (11)$$

$$a_2 * (1 + C_{33'}) + a_{2'} * (C_3 - C_{3''}) = 0 \quad (12)$$

$$-a_2 S_{33'} + a_{2'} * (S_{3''} - S_3) = 0 \quad (13)$$

Equations (11), (12) and (13) give the position constraints of the parallelogram linkage of the robot. Out of the three, two are independent, as first two of them are same. It is expected because the parallelogram linkage is planer in X-Z plane, so the constraint in y-direction does not exist.

In order to satisfy these constraints for any choice of a_2 and $a_{2'}$, it follows that

$$\theta_3 = \theta_{3''} - \theta_{2''} = \theta_{3''} \quad (14)$$

$$\theta_{3'} = \pi - \theta_3 = \pi - \theta_{3''} \quad (15)$$

Using the above equations, the vector of joint variables is q = [$\theta_{3''}$]. Therefore, the all parallelogram linkage and passive joint depend on one angle θ_2 so this linkage have only one DOF. To describe completely forward kinematics we should complete the fourth and fifth homogeneous transformation matrix, which led to get the final homogeneous transformation matrix that called arm equation.

$$A_5^3 = A_4^3 * A_5^4 \quad (16)$$

$$A_5^3 = \begin{pmatrix} C_3 C_5 & -C_{3'} C_5 & S_{3'} & a_4 C_{3'} + d_5 S_{3'} \\ S_3 C_5 & S_{3'} S_5 & -C_{3'} & a_4 S_{3'} - d_5 S_{3'} \\ -S_{3''} & -C_{3''} & 0 & Z_{3''}^0 \\ 0 & 0 & 0 & 1 \end{pmatrix} \quad (17)$$

By multiply multiple homogeneous transformation matrices, we can transform the coordinate from frame f_5 to base frame f_0, where this transform called arm equation

$$A_5^0 = arm\ equtaion = A_1^0 * A_2^1 * A_{2''}^2 * A_3^{2''} * A_4^3 * A_5^4 \quad (18)$$

When multiply the above homogeneous transformation matrices and substitute eq.14, 15 we get

$$A_5^0 = \begin{pmatrix} -C_{2-5} & -S_{2-5} & 0 & C_2 * (a_2 - a_4 + a_2 C_{3''}) \\ -S_{2-5} & C_{2-5} & 0 & S_2 * (a_2 - a_4 + a_2 C_{3''}) \\ 0 & 0 & -1 & d_1 + d_2 + d_5 - a_2 S_{3''} \\ 0 & 0 & 0 & 1 \end{pmatrix} \quad (19)$$

Where the forth column of above equation represent the position and orientation of the end effector.

$$\begin{pmatrix} P_x \\ P_y \\ P_z \end{pmatrix} = \begin{pmatrix} C_2 * (a_2 - a_4 + a_2 C_{3''}) \\ S_2 * (a_2 - a_4 + a_2 C_{3''}) \\ d_1 + d_2 + d_5 - a_2 S_{3''} \end{pmatrix} \quad (20)$$

Where Eq.(20) represent the unique forward kinematic that specialized for the climbing robot. It is clear that the θ_5 doesn't exist in arm equation, that mean this angle hasn't effect on mathematical model because this servo specialized for the gripper device only.

C. Inverse Kinematics

The inverse kinematics problem consists of the determination of the joint variables (θ_2, $\theta_{3''}$, and θ_5) corresponding to a given end effector position and orientation. The solution to this problem is the essential importance of transform the motion specifications, assigned to the end effector in the operational space, into the corresponding joint space motions that allow execution of the desired motion. In other words, the inverse kinematics problem computes the joint angles for a desired position of the end effector. There are two solutions represented by geometric and algebraic approaches used for deriving the inverse kinematics. Geometric solution approach is used for simple robot structures, such as, 2DOF arm. However, for the arms with more joints and link whose arm extends into 3DOF the geometry gets much more tedious. Hence, algebraic approach is chosen for the inverse kinematics solution for this climbing robot. At first, we suppose a matrix corresponding to the arm equation matrix Eq. (19)

$$A_5^0 = \begin{pmatrix} r_{11} & r_{12} & r_{13} & P_x \\ r_{21} & r_{22} & r_{23} & P_y \\ r_{31} & r_{32} & r_{33} & P_z \\ 0 & 0 & 0 & 1 \end{pmatrix} = A_1^0 * A_2^1 * A_{2"}^2 * A_3^{2"} * A_4^3 * A_5^4$$

(21)

To find the inverse kinematics solution for the first joint (θ_2) the link transformation inverses are premultiplied as follows

$$(A_1^0 * A_2^1)^{-1} * A_5^0 = A_{2"}^2 * A_3^{2"} * A_4^3 * A_5^4$$

(22)

Where take the inverse matrix of $A^0_1 * A^1_2$ for two side, and in the right side $[A^0_1 * A^1_2] * A^0_1 * A^1_2$ given identity matrix, so the first and second matrix of the right side should be remove. By inverse the matrix $A^0_1 * A^1_2$ and multiply them with matrix A_5^0 in the left side of Eq.(21), and equating the forth column result with the forth column of right side of the Eq.(22) yields

$$\begin{pmatrix} P_x C_2 + P_y S_2 \\ d_1 + d_2 - P_z \\ P_y C_2 - P_x S_2 \\ 1 \end{pmatrix} = \begin{pmatrix} a_2 - a_4 + a_{2'} C_3 \\ d_5 + a_{2'} S_3 \\ 0 \\ 1 \end{pmatrix}$$

(23)

From Eq.(23), we could get the angle directly using the arcos function but this function is very inaccurate for small angles. The typical way to avoid this inaccuracy is to use the atan2 function.

$$\theta_2 = a\tan 2(P_y, P_x)$$

(24)

$$\theta_3 = a\tan 2(((d_1 + d_2 + d_5 - P_z)/a_{2'}), \pm\sqrt{1 - ((d_1 + d_2 + d_5 - P_z)/a_{2'})^2})$$

(25)

$$S_5 = r_{21} * C_2 - r_{11} * S_2$$

(26)

So,

$$\theta_5 = a\tan 2(r_{21} * C_2 - r_{11} * S_2, \sqrt{1 - (r_{21} * C_2 - r_{11} * S_2)^2})$$

(27)

Where $r_{11} = -C_{2\text{-}5}$ and $r_{21} = -S_{2\text{-}5}$, $C_{2\text{-}5} = \cos(2\text{-}5)$, $S_{2\text{-}5} = \sin(2\text{-}5)$, $a_2 = 6$, $a_4 = 7$, $a_{2'} = 13$, $d_1 = 2$, $d_2 = 4$, $d_5 = 4$.

III. Climbing Robot Implementation

A. Hardware implementation

The structure of climbing robot (body and legs) is designed using AutoCAD software and then made by CNC laser machine as shown in Fig. 3.

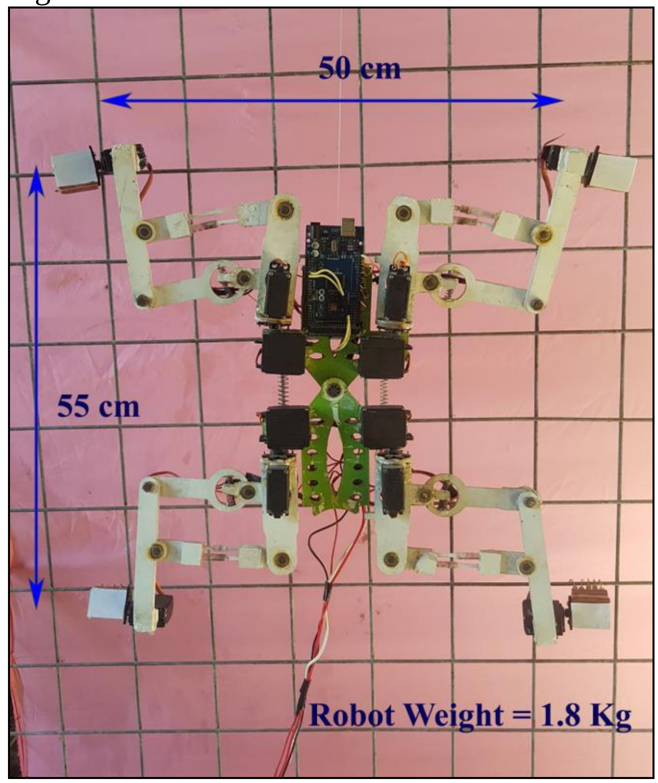

Fig. 3 climbing robot prototype climbing a mesh wall

For each arm in climbing robot, there are four rotatable joints. Each link connected with another link by joint have ball bearings that make the revolute motion more flexibility and consistency. In the parallelogram linkage, the main link is connected to the servo motor directly and it has limited moving range. This range of motion there is a spring connected in two sides of the main link, which makes the main link move a small displacement forward and backward even when the servomotor is stopping. This operation has the advantage to produce flexibility in the robot when the opposite arm move forward given the robot simplicity in the movement.

This motion is achieved by emulate the motion behavior of gecko during walking on the wall which it monitored in slow motion video. The secondary link has a passive linkage that consists of double spring give a small displacement in x-axis. This displacement used when the other arm moves forward to make a force that push the whole body in opposite direction and this force make the robot unstable and leads to falling, so this linkage will reduce the effect of this force. All springs that installed in the robot given more flexibility during climbing on the mesh wall. The three servomotors of each arm in the climbing robot are controlled by using ATmega328 microcontroller and supplied by an external power supply.

B. The design of the gripper device

As mention earlier that the robot is specialized for rough surfaces, so there is a unique design implemented for attachment to the wall by using a hooks seems like claws of cat limbs. The gripper device that connected to the servomotor M3 is made from foam material, consisting of five holes and each hole contain a spring connected to the other fishing hook. The metal cylindrical beam fixes all bases of the hooks as shown in Fig. 4.

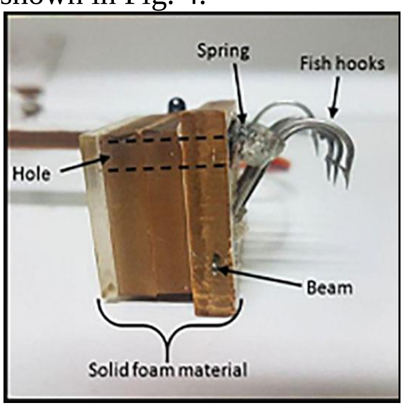

Fig. 4 the structure of the gripper device.

This design of gripper device has the benefit of making the hooks more fixable and moving in forward and backward making all the hooks reach to the wall and hang to the wall, so it gives more reliable and reduces the probability of arm fall. For more details about the design of the gripper device and the arm see our previous paper [32].

C. Locomotion principle

Initially, we will discuss the motion of one arm with a complete description of motors driving sequences. The entire arm movement consists of five movements controlled by the three servomotors with a local closed-loop controller for each motor. The motor (M1) will move the whole arm 20°outward of the wall in negative y-axis direction, and then the motor (M2) will move the arm 50° forward, after that the motor (M1) push back the whole arm to the wall again, so the arm will back to the same point in y-axis direction. For hang on the wall, the motor (M3) will rotate the gripper device 90° make a strong attachment with the wire mesh fence. The essential movement that leading the displacement upward must be performed after attachment is achieved, so the motor (M2) will pull down the arm by the degree of 50° which the whole arm will back to the same position with respect to local coordinate but with vertical upward displacement. This scenario will be performed by the other arms but starting with disengaging the attachment from a wall and repeat the previous operation again.

IV. EXPERIMENTS AND RESULTS

A. simulation results

In this section, the kinematic model will be simulated by MATLAB in order to test the arm of a climbing robot. Fig. 5 shows the rotation of the arm about z-axis due to change the value of θ_2 from the angle -20 to 0 in order to move the arm of climbing robot away from the wall which is achieved by the motor (M1) and θ_2 is evaluated by Eq.(24).

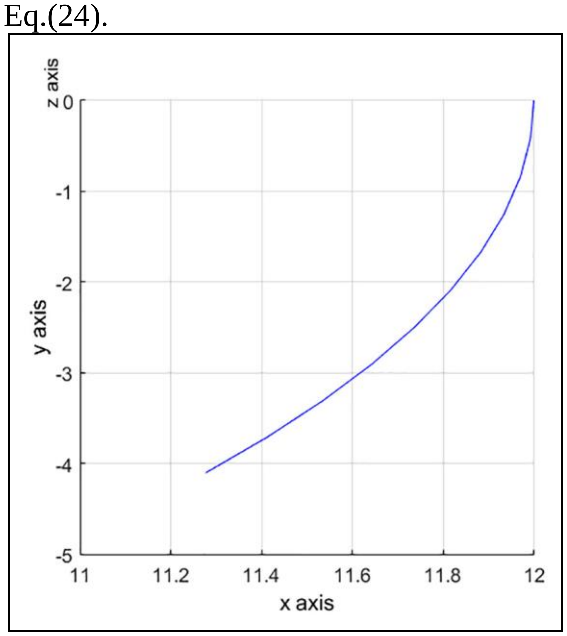

Fig. 5 Arm rotation by θ_2 angle around z-axis.

In sequence, the θ_3 rotated from the angle -20 to 20 around the y-axis which the value of θ_3 dependent on the required upward displacement and it calculated by Eq.(25). The motor (M2) achieves the rotation by θ_3. Rotation around y-axis by θ_3 value causes a small shifting in direction of x-axis, which it is 8mm as shown in Fig.6, this deviation value may not effect on the planning trajectory of the climbing robot. Whereas, the effectiveness of this shifting will appear when the range of θ_3 is not symmetric that will cause deviation in the leg trajectory and then reduce the performance of path planning of climbing robot. From Fig. 6, we can notes that the displacement in direction of z-axes is 9 cm (from 5.5° to 14.5°).

Fig. 7 shows the trajectory of a single leg of a climbing robot from the initial location to the desired coordinate by the 3D view.

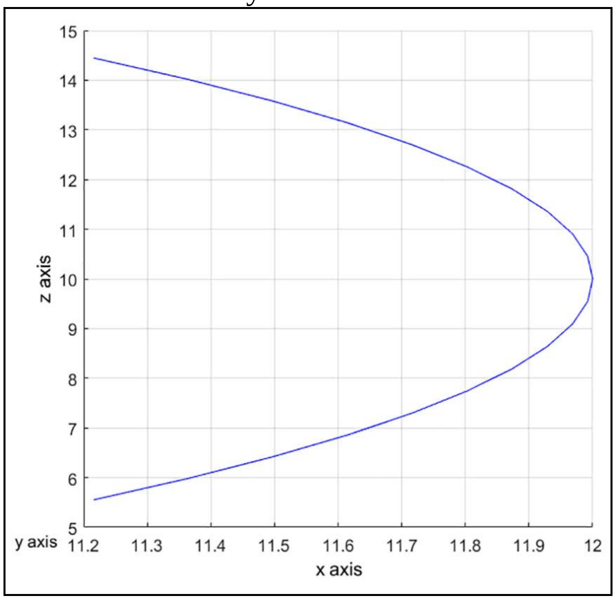

Fig. 6 Arm rotation by θ_3 angle around y-axis.

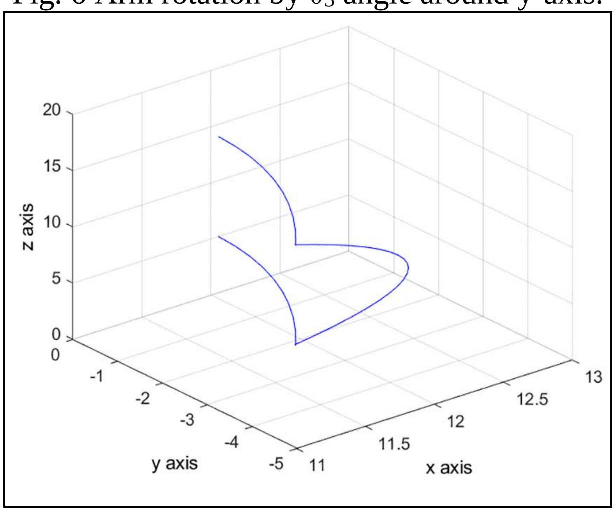

Fig. 7 Trajectory of arm of climbing robot.

In Table 1 the details about the angles and the corresponding position in the Cartesian coordinate. As mention before that, only one servomotor operate at the same time, so we see in the table that when servomotor1 operate servomotor2 in the stop state and vice versa.

TABLE I

THE ARM OF CLIMBING ROBOT POSITION WITH RESPECT TO JOINT ANGLES

Angles(in degree)		position		
θ_2	θ_3	P_x	P_y	P_z
0	0	12	0	10
-6	0	11.93	-1.25	10
-10	0	11.81	-2.08	10
-14	0	11.64	-2.9	10
-16	0	11 .53	-3.3	10
-20	0	11.27	-4.1	10
0	20	11.21	0	5.55
0	14	11.61	0	6.85
0	8	11.87	0	8.19
0	6	11.92	0	8.64
0	0	12	0	10
0	-10	11.80	0	12.25
0	-16	11.49	0	13.58
0	-20	11.21	0	14.44

B. experiment results

The practical experiments are implemented to testing the ability of the climbing robot to climb the wire mesh fence. The four limbs of climbing are controlled by 12 servomotors which MG 996R servomotor used for this propose. The servomotor has a metal gearbox, -90º to 90º rotation angle, Operating speed is 0.14 sec/60º at 6 V, and 11 kg/cm torque at 6 V supply voltage. These servomotors is controlled by robot main board, which is implemented by Atmega 328 microcontroller.

The sequence of the movement of the robot limbs are designed based on motion behavior of gecko with modification on the gecko move which is right arm and left leg moving at the same time, while in our climbing robot, the motion is starting by moving the left-hand, and then the right leg will move upward, after that the right-hand will move upward, and finally the left leg moves upward (see Fig. 8). These sequence of motion generated upward displacement with a linear speed of 0.834 cm/sec.

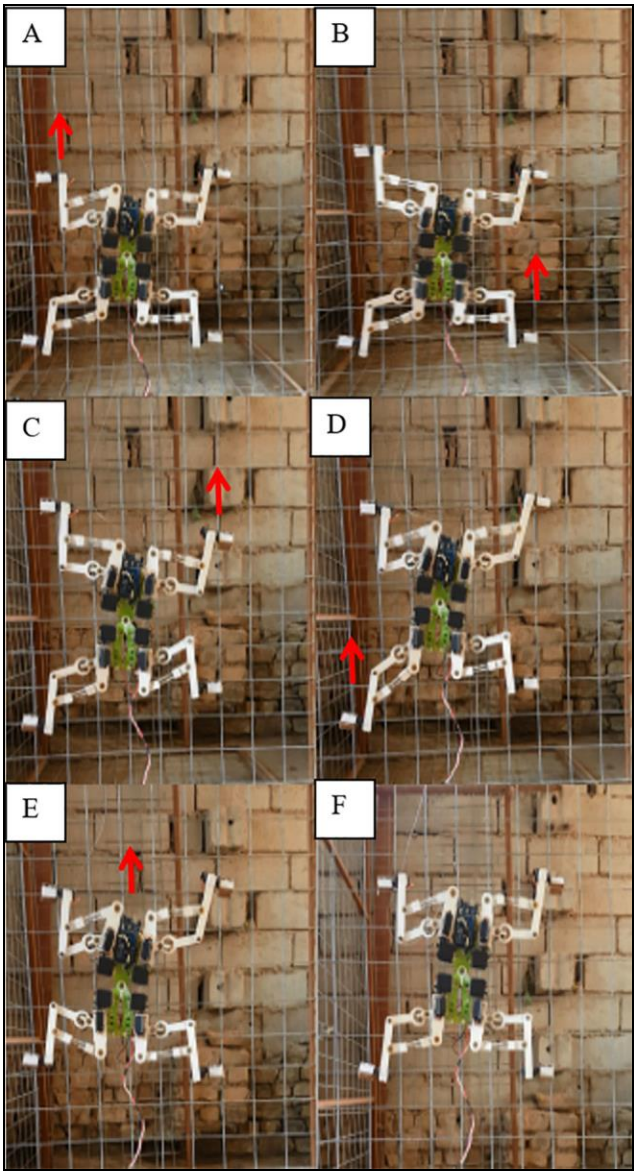

Fig. 8 The sequence of the movement of robot limbs. (A) The robot in initial position. (B) Upper left hand move upward. (C) Lower right leg move upward (D) Upper right hand move up. (E) Lower left leg moved up. (F) Return to the normal situation.

The climbing robot used the hook in the limbs as a claw for hang on the wall while the concave shape of hook help to increase the hanging force, which is the same shape of cat claw. The problem of the hang on the wall is solved by using the same behavior of cat through hang on the wall.

There is a small bend happen in the waist area of the robot that mentioned early, where this bend doesn't effect on the path of the robot because there are two spring in this area that decrease the effect of the bend. The snapshot of bend situation during body movement is shown in Fig. 9.

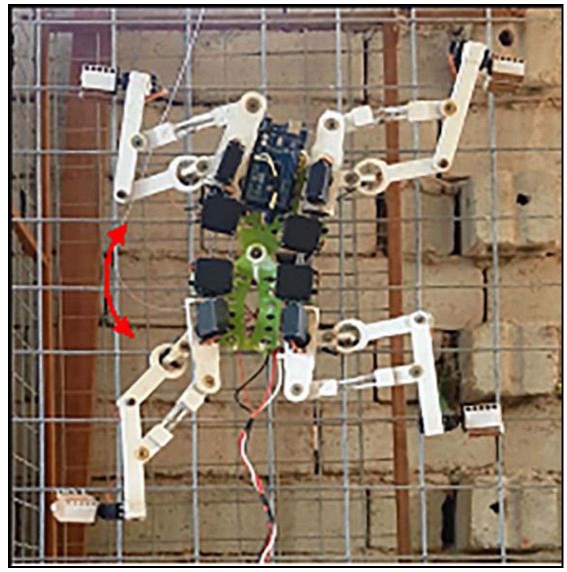

Fig. 9 The climbing robot at bending situation.

V. CONCLUSIONS

In this paper, the climbing robot is designed and implemented based on hybrid design extracted from gecko motion behavior through climbing on the wall and behavior of cat through hang on wall and trees. The kinematics model is derived for robot limbs and used for evaluation of the trajectory planning of arms of the climbing robot. The prototype of the climbing robot is designed and implemented, which several experiments performed in order to test the ability of this robot for climbing on the wire mesh fence. From the simulation results and practical experiments results, can be shown the ability of the proposed climbing robot to climbing wire mesh fence with height more than 1 m at a speed of 0.5 m/min. In addition, the claws fixed on the end of robot limbs achieved high attached force to the wall. The main controller of the robot generated perfect sequential driving signals to achieve upward movement while the internal controller inside servomotor supports the main controller of the robot.

REFERENCES

[1] Unver, O., Uneri, A., Aydemir, A., & Sitti, M. (2006, May). Geckobot: A gecko inspired climbing robot using elastomer adhesives. In Proceedings 2006 IEEE International Conference on Robotics and Automation, 2006. ICRA 2006. (pp. 2329-2335). IEEE.

[2] Murphy, M. P., & Sitti, M. (2007). Waalbot: An agile small-scale wall-climbing robot utilizing dry elastomer adhesives. IEEE/ASME transactions on Mechatronics, 12(3), 330-338.

[3] Boscariol, P., Henrey, M. A., Li, Y., & Menon, C. (2013). Optimal gait for bioinspired climbing robots using dry adhesion: a quasi-static investigation. Journal of Bionic Engineering, 10(1), 1-11.

[4] Kim, S., Spenko, M., Trujillo, S., Heyneman, B., Santos, D., & Cutkosky, M. R. (2008). Smooth vertical surface climbing with directional adhesion. IEEE Transactions on robotics, 24(1), 65-74.

[5] Li, Y., Ahmed, A., Sameoto, D., & Menon, C. (2012). Abigaille II: toward the development of a spider-inspired climbing robot. Robotica, 30(1), 79-89.

[6] Bretl, T., Rock, S., Latombe, J. C., Kennedy, B., & Aghazarian, H. (2006). Free-climbing with a multi-use robot. In Experimental Robotics IX (pp. 449-458). Springer, Berlin, Heidelberg.

[7] Shen, W., Gu, J., & Shen, Y. (2006). Permanent magnetic system design for the wall-climbing robot. Applied Bionics and Biomechanics, 3(3), 151-159.

[8] Zhang, Y., Dodd, T., Atallah, K., & Lyne, I. (2010, August). Design and optimization of magnetic wheel for wall and ceiling climbing robot. In 2010 IEEE International Conference on Mechatronics and Automation (pp. 1393-1398). IEEE.

[9] Saunders, A., Goldman, D. I., Full, R. J., & Buehler, M. (2006, May). The rise climbing robot: body and leg design. In Unmanned Systems Technology VIII (Vol. 6230, p. 623017). International Society for Optics and Photonics.

[10] Wang, S., Jiang, H., & Cutkosky, M. R. (2016, October). A palm for a rock climbing robot based on dense arrays of micro-spines. In 2016 IEEE/RSJ International Conference on Intelligent Robots and Systems (IROS) (pp. 52-59). IEEE.

[11] Parness, A., Frost, M., Thatte, N., & King, J. P. (2012, May). Gravity-independent mobility and drilling on natural rock using microspines. In 2012 IEEE International Conference on Robotics and Automation (pp. 3437-3442). IEEE.

[12] Parness, A., Abcouwer, N., Fuller, C., Wiltsie, N., Nash, J., & Kennedy, B. (2017, May). Lemur 3: A limbed climbing robot for extreme terrain mobility in space. In 2017 IEEE International Conference on Robotics and Automation (ICRA) (pp. 5467-5473). IEEE.

[13] Liu, G., Liu, Y., Wang, X., Wu, X., & Mei, T. (2016, August). Design and experiment of a bioinspired wall-climbing robot using spiny grippers. In 2016 IEEE International Conference on Mechatronics and Automation (pp. 665-670). IEEE.

[14] Sintov, A., Avramovich, T., & Shapiro, A. (2011). Design and motion planning of an autonomous climbing robot with claws. Robotics and Autonomous Systems, 59(11), 1008-1019.

[15] Funatsu, M., Kawasaki, Y., Kawasaki, S., & KikuchiI, K. (2014, August). Development of cm-scale wall climbing hexapod robot with claws. In Proceedings of the 3rd International Conference on Design Engineering and Science—ICDES, Pilsen, Czech Republic (pp. 101-106).

[16] Bryant, M., Fitzgerald, J., Miller, S., Saltzman, J., Kim, S., Lin, Y., & Garcia, E. (2014, March). Climbing robot actuated by meso-hydraulic artificial muscles. In Active and Passive Smart Structures and Integrated Systems 2014 (Vol. 9057, p. 90570H). International Society for Optics and Photonics.

[17] Ji, A., Zhao, Z., Manoonpong, P., Wang, W., Chen, G., & Dai, Z. (2018). A bio-inspired climbing robot with flexible pads and claws. Journal of Bionic Engineering, 15(2), 368-378.

[18] Jiang, Q., & Xu, F. (2017). Grasping Claws of Bionic Climbing Robot for Rough Wall Surface: Modeling and Analysis. Applied Sciences, 8(1), 14.

[19] Miller, B., Clark, J., & Darnell, A. (2013, May). Running in the horizontal plane with a multi-modal dynamical robot. In 2013 IEEE International Conference on Robotics and Automation (pp. 3335-3341). IEEE.

[20] Xu, F., Wang, B., Shen, J., Hu, J., & Jiang, G. (2018). Design and realization of the claw

gripper system of a climbing robot. Journal of Intelligent & Robotic Systems, 89(3-4), 301-317.

[21]Xu, F., Wang, X., & Jiang, G. (2012). Design and analysis of a wall-climbing robot based on a mechanism utilizing hook-like claws. International Journal of advanced robotic systems, 9(6), 261.

[22]Li, X., Wang, W., Wu, S., Zhu, P., Zhao, F., & Wang, L. (2018). The gait design and trajectory planning of a gecko-inspired climbing robot. Applied bionics and biomechanics, 2018.

[23]Zhu, P., Wang, W., Wu, S., Li, X., & Meng, F. (2016, December). Configuration and trajectory optimization for a Gecko Inspired climbing robot with a Pendular waist. In 2016 IEEE International Conference on Robotics and Biomimetics (ROBIO) (pp. 1870-1875). IEEE.

[24]Wolfram Burgard; Oliver Brock; Cyrill Stachniss, "Design of a Bio-inspired Dynamical Vertical Climbing Robot," in Robotics: Science and Systems III , , MITP, 2008, pp.

[25] Wang, W., Wu, S., Zhu, P., & Liu, R. (2015, September). Analysis on the dynamic climbing forces of a gecko inspired climbing robot based on GPL model. In 2015 IEEE/RSJ International Conference on Intelligent Robots and Systems (IROS) (pp. 3314-3319). IEEE.

[26]Haynes, G. C., Khripin, A., Lynch, G., Amory, J., Saunders, A., Rizzi, A. A., & Koditschek, D. E. (2009, May). Rapid pole climbing with a quadrupedal robot. In 2009 IEEE International Conference on Robotics and Automation (pp. 2767-2772). IEEE.

[27]Lam, T. L., & Xu, Y. (2012). A novel tree-climbing robot: treebot. In Tree Climbing Robot (pp. 23-54). Springer, Berlin, Heidelberg.

[28]Lam, T. L., & Xu, Y. (2011). Climbing strategy for a flexible tree climbing robot—treebot. IEEE Transactions on Robotics, 27(6), 1107-1117.

[29]Palmer III, L. R., Diller, E., & Quinn, R. D. (2015). Toward gravity-independent climbing using a biologically inspired distributed inward gripping strategy. IEEE/ASME Transactions on Mechatronics, 20(2), 631-640.

[30]Denavit, J. (1955). A kinematic notation for low pair mechanisms based on matrices. ASME J. Appl. Mech., 22, 215-221.

[31] Siciliano, B., Sciavicco, L., Villani, L., & Oriolo, G. (2010). Robotics: modelling, planning and control. Springer Science & Business Media.

[32]Hassan, M. Y., Rashid, M. T., & Abdulaali, A. H. Design and Implementation of Hybrid Arm for the Climbing Robot. International Journal of Computer Applications, 975, 8887.